Applied Physics Letters

Pulsed- and continuous-mode operation at high temperature of strained quantum-cascade lasers grown by metalorganic vapor phase epitaxy

Cite as: Appl. Phys. Lett. **88**, 041102 (2006); https://doi.org/10.1063/1.2166206
Submitted: 19 August 2005 . Accepted: 23 November 2005 . Published Online: 23 January 2006

L. Diehl, D. Bour, S. Corzine, J. Zhu, G. Höfler, B. G. Lee, C. Y. Wang, M. Troccoli, and F. Capasso

Pulsed- and continuous-mode operation at high temperature of strained quantum-cascade lasers grown by metalorganic vapor phase epitaxy

L. Diehl[a)]
Harvard University, Division of Engineering and Applied Science, Cruft Laboratory 310, 19 Oxford Street, Cambridge, Massachusetts 02138

D. Bour, S. Corzine, J. Zhu, and G. Höfler
Agilent Laboratories, Photonics and Electronics Research Laboratory, 3500 Deer Creek Road, Palo Alto, California 94304

B. G. Lee, C. Y. Wang, M. Troccoli, and F. Capasso
Harvard University, Division of Engineering and Applied Science, Cruft Laboratory 310, 19 Oxford Street, Cambridge, Massachusetts 02138

(Received 19 August 2005; accepted 23 November 2005; published online 23 January 2006)

We present the pulsed operation at room temperature of different strained InGaAs/AlInAs quantum-cascade lasers grown by low-pressure metalorganic vapor-phase epitaxy. Devices based on a bound-to-continuum transition design have threshold current densities in pulsed mode as low as 1.84 kA/cm^2 at 300 K. Identical lasers grown at higher rate (0.5 nm/s) also have threshold current densities lower than 2 kA/cm^2 at 300 K. Buried heterostructure lasers based on a double phonon resonance design were operated in continuous mode up to 280 K. Overall, the performance obtained from strained quantum cascade lasers deposited by metalorganic vapor-phase epitaxy are comparable with that of similar structures grown by molecular beam epitaxy. © *2006 American Institute of Physics*. [DOI: 10.1063/1.2166206]

Quantum cascade lasers (QCLs) are the light source of choice for many potential applications such as gas sensing in the midinfrared.[1] State-of-the-art QCLs have indeed demonstrated large tunability, low-threshold, and high-power in continuous mode (cw) at room temperature.[2,3] The devices which exhibit the best performance have been so far grown by molecular beam epitaxy (MBE). This fabrication technique provides several advantages, such as the ease to form abrupt interfaces, but is not suitable for low-cost, high throughput production. On the contrary, low-pressure metalorganic vapor-phase epitaxy (MOVPE) is a well-established technology fitting the requirements of large scale production, especially since high growth rates are possible.[4–6] However, it is still necessary to demonstrate that MOVPE- and MBE-grown QCLs can have similar performance particularly since the control of interface abruptness is more challenging by MOVPE. QCLs fabricated using the latter technique have already been operated recently at room-temperature in pulsed mode. The threshold current densities for these lattice-matched devices were low, i.e., between 2.4 and 3 kA/cm^2 at 300 K and the emission wavelength longer than 7.2 μm.[4,6] Structures at shorter wavelengths require in order to achieve high performance at room temperature, the use of strain-balanced material because of the large band discontinuity available.[7]

This letter reports on the fabrication of strained QC lasers grown by MOVPE working in pulsed mode above 320 K. Threshold current density as low as 1.84 kA/cm^2 at 300 K and characteristic temperature T_0 close to 200 K were obtained from devices based on a bound-to-continuum design. Another sample based on a double phonon resonance design worked in cw up to 280 K. More than 80 mW output power was delivered by the device in cw mode at 243 K.

Three strained QC structures were deposited on highly doped substrate by low pressure (76 Torr) MOVPE. The parameters were identical to those used for the growth of the lattice-matched QCLs reported in Refs. 5 and 6. The flows of triethylgallium and trimethylaluminium were simply adjusted to form the strained $In_{0.6}Ga_{0.4}As$ and $Al_{0.56}In_{0.44}As$ alloys. The active region of the first two samples investigated is based on a bound-to-continuum design previously reported by Blaser *et al.*[3] and was deposited at a slow (0.1 nm/s) and a fast (0.5 nm/s) rate. The doping in the injector was kept low (1×10^{17} cm^3) to limit the waveguide losses. Thirty stages were grown and embedded between 0.3-μm-thick In–GaAs guiding layers doped 3×10^{16} cm^3, in addition to 3-μm-thick InP cladding layers doped 1×10^{17} cm^3. Step-graded 30-nm-thick InGaAsP layers were inserted at the InP–InGaAs interfaces to reduce series resistance. The growth ended with a 0.5-μm-thick InP layer doped 1×10^{19} cm^3 for plasmon-enhanced optical confinement and reduced losses, followed by highly doped contact layers. The deposition rate, except in the active region was kept constant at a value of 0.5 nm/s. The third structure studied in this letter replicates the lasers described in Refs. 8 and 9 based on a double phonon resonance design. Our sample comprises 30 stages and the waveguide is similar to the one described earlier.

Figure 1 shows the x-ray diffraction spectra of the two QCLs based on a bound-to-continuum design, together with the results of simulations. The comparison between the different patterns clearly shows very similar diffraction spectra, no noticeable degradation of the crystal quality as the growth rate changes and an excellent reproducibility of the structure

[a)]Electronic mail: ldiehl@deas.harvard.edu

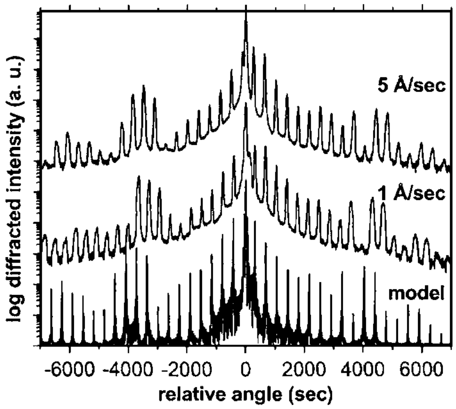

FIG. 1. Comparison between simulations and x-ray diffraction spectra of the fast- and slow-grown bound-to-continuum QCL measured along the (004) crystal direction. The curves are shifted for clarity.

from one run to the other. For both samples, the zeroth order peak due to the periodicity of the superlattice is very close to the InP substrate peak, which indicates only a slight lattice mismatch in the structures. The average length of the QC stages can be deduced from the different spectra. The period of the active region is 49.3 and 49.7 nm for the slow- and fast-grown structures, respectively, which is in both cases thinner than the targeted thickness (50.6 nm). This observation is consistent with the fact that the emission wavelength of our lasers is blueshifted with respect to the original design [4.98 μm vs 5.4 μm, see the inset of Fig. 2(a)].

Ridge waveguide lasers were fabricated using conventional processing techniques. The samples were cleaved manually, soldered ridge side-up with indium onto gold-plated copper heatsinks and finally wire bonded. After fabrication, the lasers were mounted into a temperature-controlled LN_2-cooled flow cryostat. Current pulses (163 ns) at a frequency of 92 kHz, corresponding to a duty cycle of 1.5%, were supplied to the lasers. For measurements in continuous mode, the devices were mounted on a Peltier cooler installed in a purged box. The light from the laser facet was collected by $f/1$ optics and sent either onto a calibrated thermopile detector for power measurements or into a Fourier-transform infrared spectrometer equipped with a deuterated triglycine sulphate detector for spectral characterization.

Figure 2(a) shows the voltage and the light-intensity versus current (*VI* and *LI*) curves of a 1.9-mm-long and 16-μm-wide laser fabricated from the slow-grown material. The maximum emitted peak power was 156 and 51 mW with a slope efficiency dP/dI equal to 564 and 380 mW/A at, respectively, 243 and 300 K. The inset of Fig. 2(a) shows typical spectra obtained close to threshold.

The threshold current density j_{th} measured in pulsed mode is plotted as function of temperature in Fig. 2(b) for the fast- and slow-grown samples. In both cases, the lasers worked at temperatures above 320 K and the characteristic temperature T_0, which describes the behavior of the threshold current versus temperature was close to 200 K. For the slow-grown device, j_{th} ranges from 1.39 to 2.07 kA/cm^2 between 243 and 320 K and is close to the values obtained in Ref. 3. In this letter indeed, a threshold current density of 1.38 kA/cm^2 was reported for a 3-mm-long device operated in continuous mode at a heatsink temperature T_{sink} of 243 K. The latter corresponds to a temperature in the active region $T_{\mathrm{act}}=T_{\mathrm{sink}}+T_{\mathrm{elec}}\cdot R_{\mathrm{th}}$ close to 266 K, given the electric power

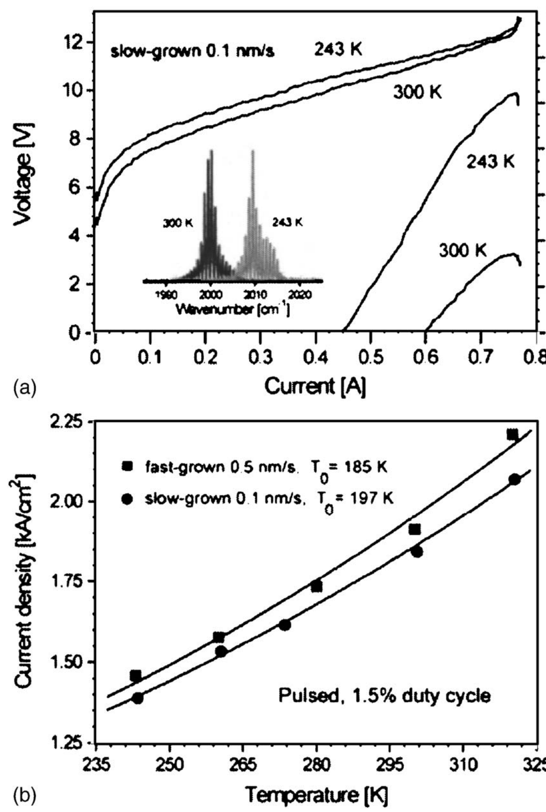

FIG. 2. Summary of the data obtained with the lasers based on a bound-to-continuum transition design in pulsed mode. (a) *VI*/*LI* curves and optical spectra close to threshold (inset) taken at 243 and 300 K with the slow grown sample. (b) Threshold current density vs temperature for the slow- and fast-grown QCLs. Note that the latter has a cavity length 31% longer than the slow-grown laser. The curves correspond to the usual exponential fit $j_{\mathrm{th}}=j_0\exp(T/T_0)$.

P_{elec} of 3.75 W and the thermal resistance of R_{th} 6.3 K/W measured by Blaser *et al.* Assuming that heating effects are negligible in pulsed mode, we can expect for their device a pulsed threshold of 1.38 kA/cm^2 at about 266 K. This is only 15% lower than the threshold current density of the slow-grown QCL investigated in the present letter. This difference would be even smaller lasers of equal length were compared.

As shown in Fig. 2(b), the threshold current density of the fast-grown lasers is less than 2 kA/cm^2 up to 304 K and the characteristic temperature T_0 reaches 185 K. This result is remarkable given the high deposition rate (0.5 nm/s) used during the growth of the sample. However, the difference in terms of performance between the slow- and fast-grown QCLs is not negligible, although the curves in Fig. 2(b) suggest the contrary. It is due to the fact that the cavity length of the fast-grown QCL was longer (2.52 mm) than in the case of the slow-grown sample. If both lasers would have been cleaved in exactly 2-mm-long bars, the difference in threshold current density would be about 20% higher. Note that the measured slope efficiency is only 232 mW/A for the fast grown samples.

The QC sample based on a double phonon resonance design was processed into narrow-stripe buried heterostructure lasers. In this case, the active region is surrounded by insulating InP doped with Fe, lowering the thermal resistance of the device and allowing continuous wave operation at high temperatures. To reduce the thermal resistance even fur-

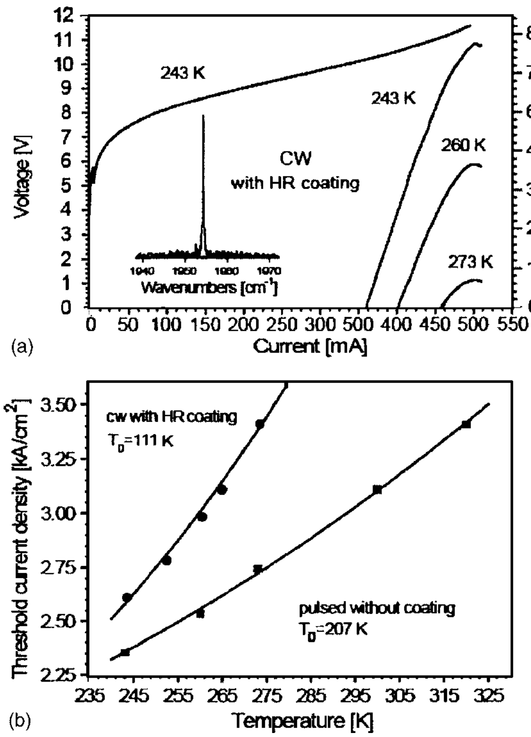

FIG. 3. Summary of the data obtained with the structure based on a four quantum wells transition design in pulsed and continuous mode. (a) *VI* and *LI* taken at different temperatures in continuous mode after the evaporation of a HR coating on the backfacet. The inset shows the optical spectra measured close to threshold at 243 K. (b) Threshold current density as a function of the heatsink temperature in pulsed and continuous mode, respectively without and with a high-reflection coating. The curves correspond to the usual exponential fit $j_{th}=j_0 \exp(T/T_0)$.

ther, a thick layer of gold was electroplated onto the usual Ti/Au top contact. The best results were obtained with a 7-μm-wide and 2-mm-long laser mounted junction-up, which operated at temperatures above 320 K in pulsed mode. The measured slope efficiency with a 1.5% duty cycle reached 636 mW/A at 243 K and 339 mW/A at 320 K. The device could be operated in continuous mode at 243 K. The temperature range accessible was, however, limited since the cw threshold current density (3.29 kA/cm^2 at 243 K) was fairly close to the injection current at which the roll-over of the output power takes place (3.74 kA/cm^2 at 243 K). The maximum intensity was 6.6 mW and the slope efficiency 172 mW/A. A high-reflection (HR) coating consisting of 175 nm Al_2O_3 and 30 nm Au was deposited on the backfacet of the laser and helped to reduce the cw threshold current density. The value of the latter dropped to 2.61 kA/cm^2 at 243 K and the maximum cw temperature operation of the laser increased up to 280 K. Figure 3(a) shows the cw *VI-LI* curves of the device after the evaporation of the HR coating. The intensity reached 81 mW (dP/dI=657 mW/A) at 243 K and was still 8 mW (dP/dI =257 mW/A) at 273 K. The inset of Fig. 3(a) shows a typical spectrum obtained if the laser is operated slightly above threshold in cw mode. At 243 K, the emission wavelength is 1954 cm^{-1} (5.11 μm), which is in quite good agreement with the expected value of (5.3 μm).[8]

The threshold current densities obtained in pulsed and cw mode at different temperatures are displayed in Fig. 3(b). Note that the measurements shown were taken without (pulsed mode) and with (cw) the HR coating on the backfacet of the laser. From an exponential fit of the data, the characteristic temperature T_0 can be deduced. It yields 207 and 111 K in pulsed and cw mode, respectively. The thermal resistance R_{th} of the device can be estimated at 243 K by comparing the threshold current density in cw obtained without HR coating (3.29 kA/cm^2) and the pulsed measurements displayed in Fig. 3(b). This leads to a value of R_{th} equal to 14.5 K/W corresponding to a thermal conductance G_{th} =516 W/K cm^{-2}. From the change of current density before and after the deposition of the HR coating, the waveguide losses can be estimated and yield 9.7 cm^{-1}. The performances reported in Figs. 3(a) and 3(b) are similar to those reported in Refs. 8 and 9 although a direct comparison is not as straight-forward as in the case of the bound-to-continuum samples. Slightly lower performance is however, anticipated for the MOVPE-grown lasers since the linewidth of the electroluminescence peak measured at room temperature is broader (36 meV) than the corresponding value (25 meV) found in Ref. 8 and 9.

In conclusion our results demonstrate the realization of strained QCLs based on a bound-to-continuum design which operate in pulsed mode above 320 K with a very low threshold current density. Devices based on a double phonon resonance design and processed into buried heterostructures lasers worked in continuous wave up to 280 K. The results presented in this letter are comparable with those of equivalent structures grown by molecular beam epitaxy. The performance level can be improved in many ways, including the optimization of the processing of buried heterostructure devices as well as the doping in the active region. It will allow without doubts the cw operation at 300 K of these lasers. Another remarkable finding is the low threshold current densities (less than 2 kA/cm^2) measured at room temperature with lasers deposited at a high growth rate of 0.5 nm/s. Altogether, the results presented in this letter demonstrate that MOVPE is a viable solution to grow high performance low-threshold strained QCLs operating in cw at room temperature.

The Harvard group acknowledges partial financial support from Agilent Technologies, from the U.S. Army Research Laboratory and the U.S. Army Research Office under Grant No. W911NF-04-1-0253. Part of the processing was done at the Center for Nanoscale Systems (CNS) at Harvard University. Harvard-CNS is a member of the National Nanotechnology Infrastructure Network (NNIN).

[1]A. Kosterev and F. Tittel, IEEE J. Quantum Electron. **38**, 582 (2002).
[2]J. Yu, S. Slivken, S. Darvish, A. Evans, B. Gokden, and M. Razeghi, Appl. Phys. Lett. **87**, 041104 (2005).
[3]S. Blaser, D. Yarekha, L. Hvozdara, Y. Bonetti, A. Muller, M. Giovannini, and J. Faist, Appl. Phys. Lett. **86**, 41109 (2005).
[4]R. P. Green, L. R. Wilson, E. A. Zibik, D. G. Revin, J. W. Cockburn, C. Pflügl, W. Schrenk, G. Strasser, A. B. Krysa, J. S. Roberts, C. M. Tey, and A. G. Cullis, Appl. Phys. Lett. **85**, 5529 (2004).
[5]D. Bour, M. Troccoli, F. Capasso, S. Corzine, A. Tandon, D. Mars, and G. Höfler, J. Cryst. Growth **272**, 526 (2004).
[6]M. Troccoli, D. Bour, S. Corzine, G. Höfler, A. Tandon, D. Mars, D. Smith, L. Diehl, and F. Capasso, Appl. Phys. Lett. **85**, 5842 (2004).
[7]J. Faist, F. Capasso, D. Sivco, A. Hutchinson, S. Chu, and A. Cho, Appl. Phys. Lett. **72**, 680 (1998).
[8]D. Hofstetter, M. Beck, T. Aellen, and J. Faist, Appl. Phys. Lett. **78**, 396 (2001).
[9]D. Yarekha, M. Beck, S. Blaser, T. Aellen, E. Gini, D. Hofstetter, and J. Faist, IEEE Electron Device Lett. **39**, 1123 (2003).